Journal Pre-proof

Fluorescent gold nanocluster-based sensor for detection of alkaline phosphatase in human osteosarcoma cells

Hao-Hua Deng, Qi Deng, Ke-Lin Li, Qiong-Qiong Zhuang, Yu-Bin Zhuang, Hua-Ping Peng, Xing-Hua Xia, Wei Chen

PII: S1386-1425(19)31265-X

DOI: https://doi.org/10.1016/j.saa.2019.117875

Reference: SAA 117875

To appear in: *Spectrochimica Acta Part A: Molecular and Biomolecular Spectroscopy*

Received date: 19 October 2019

Revised date: 27 November 2019

Accepted date: 28 November 2019

Please cite this article as: H.-H. Deng, Q. Deng, K.-L. Li, et al., Fluorescent gold nanocluster-based sensor for detection of alkaline phosphatase in human osteosarcoma cells, *Spectrochimica Acta Part A: Molecular and Biomolecular Spectroscopy*(2019), https://doi.org/10.1016/j.saa.2019.117875

Fluorescent gold nanocluster-based sensor for detection of alkaline phosphatase in human osteosarcoma cells

Hao-Hua Deng,[a#] Qi Deng,[b#] Ke-Lin Li,[a] Qiong-Qiong Zhuang,[a] Yu-Bin Zhuang,[c] Hua-Ping Peng,*[a] Xing-Hua Xia,[d] Wei Chen*[a]

[a] Higher Educational Key Laboratory for Nano Biomedical Technology of Fujian Province, Department of Pharmaceutical Analysis, Fujian Medical University, Fuzhou 350004, China

[b] Fujian Key Laboratory of Drug Target Discovery and Structural and Functional Research, School of Pharmacy, Fujian Medical University, Fuzhou 350004, China

[c] Laboratory Animal Center, Fujian Medical University, Fuzhou 350004, China

[d] State Key Laboratory of Analytical Chemistry for Life Science and Collaborative Innovation Center of Chemistry for Life Sciences, School of Chemistry and Chemical Engineering, Nanjing University, Nanjing 210093, China

* Corresponding author. Tel./fax: +86 591 22862016.

E-mail address: chenandhu@163.com (W. Chen), phpfjmu@126.com (H.P. Peng).

[#] Hao-Hua Deng and Qi Deng contributed equally to this work.

Abstract

Gold nanoclusters (AuNCs) have attracted much attention as signal transducers in photoluminescence chemical/biological sensors. Herein, we employ bovine serum albumin/3-mercaptopropionic acid co-modified AuNCs as a fluorescence probe, Fe^{3+} as a quencher, and pyrophosphate as an alkaline phosphatase (ALP) substrate and Fe^{3+} chelator to design a novel biosensor for ALP detection, achieving a detection linear range of 0.8–16 U/L and a detection limit of 0.78 U/L. The developed method is successfully applied to the detection of ALP in human osteosarcoma cells and is shown to be suited for ALP inhibitor screening.

Keywords: Gold nanocluster; Fluorescence; Alkaline phosphatase; Human osteosarcoma cells; Enzyme inhibitor

1. Introduction

Alkaline phosphatase (ALP, EC 3.1.3.1), a membrane-bound metalloenzyme, is widely distributed in human tissues such as liver, bone, intestine, kidney, and placenta [1, 2]. Under alkaline conditions, ALP can catalyze the hydrolysis of inorganic pyrophosphate (PPi) to phosphate (Pi) and the de-/transphosphorylation of other phosphate ester-containing molecules, thus playing an important role in cellular signal transduction and cell cycle (growth and apoptosis) regulation. ALP is a widely used biomarker for clinical diagnosis and therapy, as its abnormal expression is associated with numerous diseases such as liver dysfunction [3], bone disease [4], and prostate cancer [5]. Moreover, ALP is a widely used label in gene- and immunoassays for nucleic acid, proteins, and drug monitoring. Therefore, the development of convenient, sensitive, and selective ALP detection methods is a task of high significance [6-8].

Gold nanoclusters (AuNCs) are relatively stable molecular aggregates comprising several to hundreds of gold atoms protected by an organic molecule layer [9]. As the sizes of AuNCs are comparable to the Fermi wavelength of internal electrons, the continuous energy level near the Fermi level splits into discrete energy levels to endow these nanoclusters with physicochemical and photoelectric properties different from those of nanoparticles, as exemplified by unique HOMO-LUMO transitions [10],

magnetism [11], optical isomerism [12], photocatalytic activity [13], photoluminescence [14, 15], and electrochemiluminescence [16, 17]. Compared with traditional fluorescent materials such as small-molecular organic fluorescent dyes, quantum dots, and fluorescent proteins, AuNCs feature the advantages of high photostability, adjustable fluorescence wavelength, good biocompatibility, and preparation simplicity, and are therefore widely used for small molecule and protein detection as well as for cell labeling and imaging [18-30].

In our previous work, 3-mercaptopropionic acid (MPA) and bovine serum albumin (BSA) were employed as co-modifiers to prepare water-soluble BSA/MPA-AuNCs with orange-yellow fluorescence [31], which was found to be effectively and selectively quenched by Fe^{3+}. Herein, the combination of Fe^{3+}-induced quenching of BSA/MPA-AuNC fluorescence and the PPi-triggered fluorescence recovery is used to detect ALP in human osteosarcoma cells. The developed method is shown to be suitable for the screening of alkaline phosphatase inhibitors and is concluded to have great application prospects in biological research and clinical diagnosis.

2. Materials and methods

2.1. Materials and instruments

$HAuCl_4 \cdot 4H_2O$ and $FeCl_3 \cdot 6H_2O$ were purchased from Aladdin Reagent Co. (Shanghai, China). BSA was obtained from Sinopharm Chemical Reagent Co., Ltd. (Shanghai, China). MPA was acquired from Adamas Reagent Co. (Shanghai, China). Sodium pyrophosphate and ALP were procured from Sigma-Aldrich (Shanghai, China). Photoluminescence spectra were recorded on a Cary Eclipse fluorescence spectrophotometer (Agilent, USA). Transmission electron microscopy (TEM) images were acquired on a JEM-2100 microscope (JEOL, Japan).

2.2 ALP detection procedure

Tris-HCl buffer (pH 9.1; 10 mM, 100 μL) was treated with aqueous sodium pyrophosphate (150 μM, 100 μL) and varying amounts of ALP, and the obtained mixture was incubated at 37 °C for 30 min, treated with aqueous HAc (0.7 M, 180 μL)

and BSA/MPA-AuNCs-Fe^{3+} (120 μL), and incubated for 10 min at 37 °C. After the reaction, the fluorescence intensity at 575 nm (F_{575}) was measured using an excitation wavelength of 320 nm.

2.3. ALP detection in human osteosarcoma cells

Human bone osteosarcoma cells (Saos-2) were grown in McCoy's 5A complete medium supplied with fetal bovine serum (10%), streptomycin sulfate (100 U/mL), penicillin G sodium (100 U/mL), and L-glutamine (2 mM) for 24 h at 37 °C. Triton X-100 solution (0.01%, 100 μL) was added to each cell well, which was followed by incubation on ice upon continuous shaking for 30 min. The cell lysate was centrifuged at 12000 rpm for 10 min at 4 °C, and 100 μL of the supernatant was collected for the ALP assay.

2.4. Evaluation of the inhibitory effect of NaF on ALP activity

NaF solutions (50 μL) of different concentrations were added to sodium pyrophosphate (300 μM, 50 μL) and ALP (100 U/L, 100 μL) solutions, and the mixtures were incubated at 37 °C for 30 min and treated with HAC (0.7 M, 180 μL) and BSA/MPA-AuNCs-Fe^{3+} (120 μL). The F_{575} (320-nm excitation) of the resulting mixtures was measured after 10-min incubation at 37 °C.

3. Results and discussion

3.1. Principle of ALP biosensing

Highly fluorescent BSA/MPA-AuNCs were prepared according to a previously published protocol [32] and had diameters of <2 nm (Fig. 1A). The colorless and transparent BSA/MPA-AuNC aqueous solution exhibited intense orange-yellow fluorescence under irradiation with ultraviolet light (Fig. 1B), with maximum excitation and emission wavelengths determined as 360 and 575 nm, respectively.

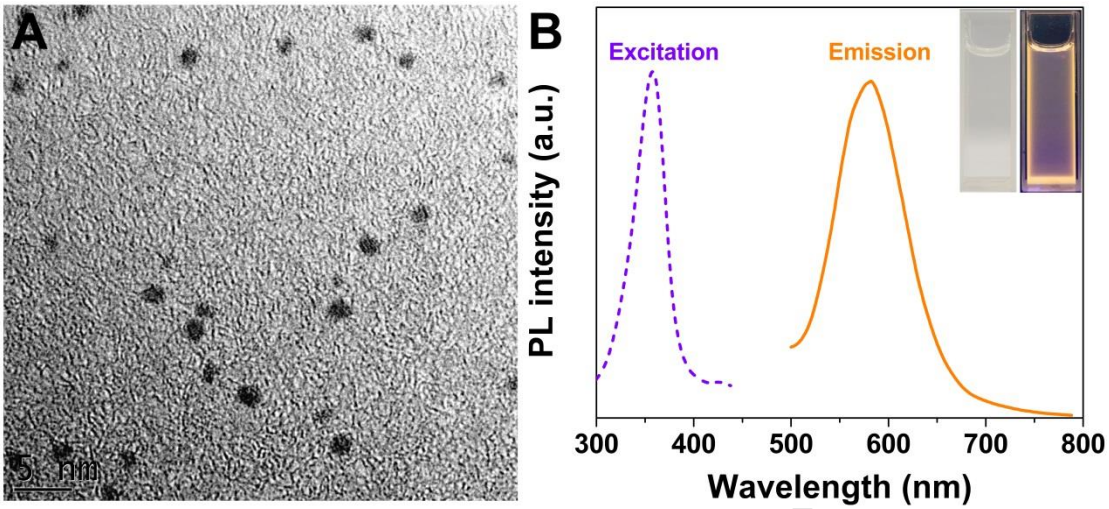

Fig. 1. (A) Representative TEM image and (B) fluorescence spectra of BSA/MPA-AuNCs. Inset in (B) shows photographs of BSA/MPA-AuNCs in ambient light (left) and UV light (right). The scale bar represents 5 nm.

In the presence of Fe^{3+}, the fluorescence of BSA/MPA-AuNCs significantly decreased (turn-off) (Fig. 2), which was ascribed to the fact that the semi-full state of the Fe 3d orbitals ($4s^2 3d^5$) resulted in relatively high electron density and strong electron-transfer ability [33]. Therefore, upon exposure to BSA/MPA-AuNCs, Fe^{3+} rapidly bound to MPA, and the d-orbital electron transfer resulted in fluorescence quenching [32]. The introduction of PPi resulted in the restoration of fluorescence (turn-on) due to the competitive binding of PPi to Fe^{3+}. In the presence of ALP, PPi was hydrolyzed to release Fe^{3+}, and the fluorescence was turned off. The conceptual framework of the proposed ALP biosensor is shown in Scheme 1.

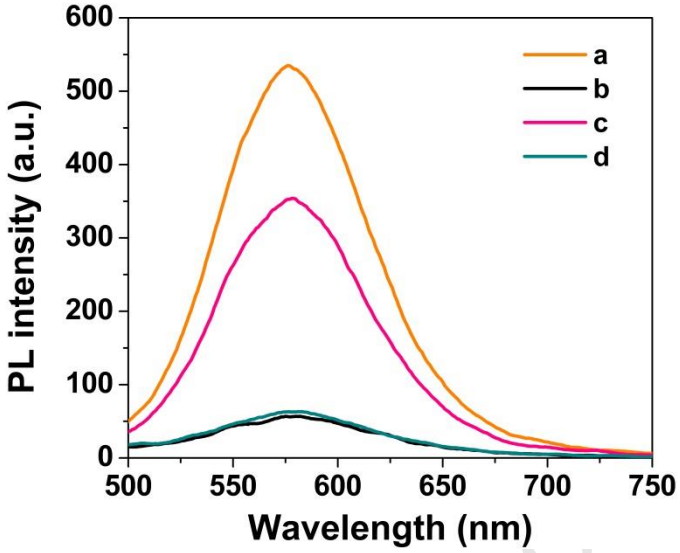

Fig. 2. Fluorescence emission spectra of (a) BSA/MPA-AuNCs, (b) BSA/MPA-AuNCs + 10 μM Fe^{3+}, (c) BSA/MPA-AuNCs + 10 μM Fe^{3+} + 30 μM PPi, and (d) BSA/MPA-AuNCs + 10 μM Fe^{3+} + 30 μM PPi + 40 U/L ALP.

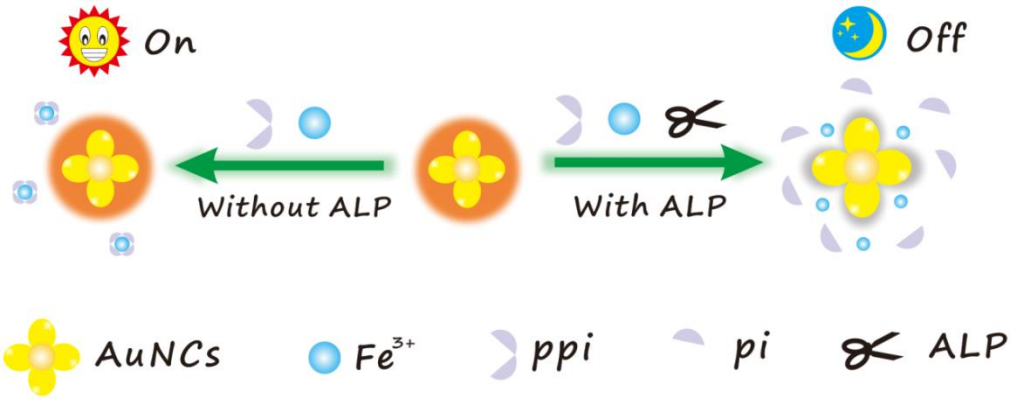

Scheme 1. Schematic illustration of fluorescent ALP biosensing based on BSA/MPA-AuNCs and an enzyme-triggered reaction.

3.2. Optimization of detection conditions

After proving the feasibility of our method, we optimized assay conditions. First, the effect of Fe^{3+} concentration on the emission performance of BSA/MPA-AuNCs was investigated. As shown in Fig. 3A, F_{575} decreased with increasing Fe^{3+} concentration, reaching a plateau at 10 μM, which was therefore chosen as the optimal Fe^{3+} concentration. Next, we optimized the concentration of sodium pyrophosphate. As can be seen from Fig. 3B, F_{575} increased with increasing sodium pyrophosphate

concentration, saturating at concentrations higher than 30 μM. Therefore, the optimum concentration of sodium pyrophosphate was chosen as 30 μM.

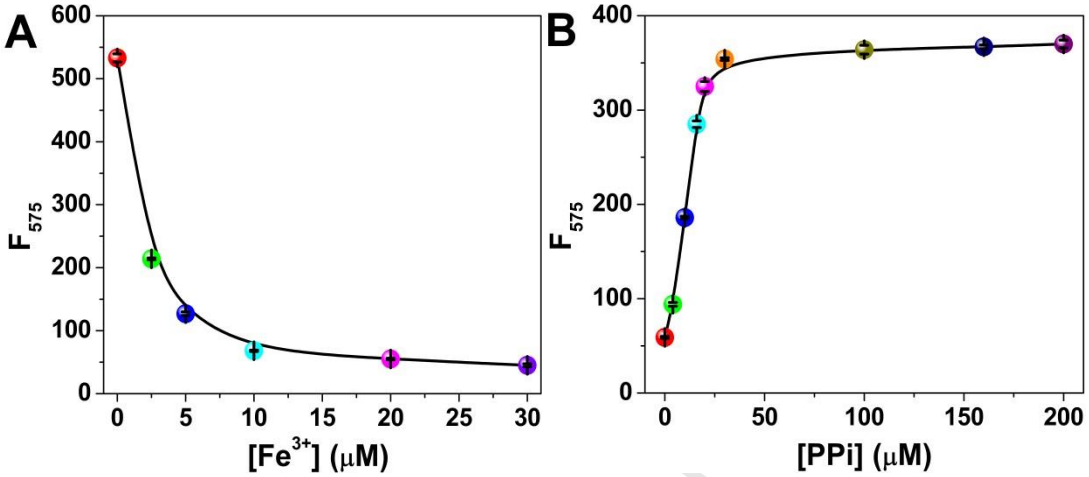

Fig. 3. Dependence of F_{575} on the concentrations of (A) Fe^{3+} and (B) sodium pyrophosphate. The concentration of BSA/MPA-AuNCs is 0.2 mM (based on Au content).

3.3. ALP assay performance

The performance of the proposed biosensor was investigated for various concentration of ALP under optimized conditions. F_{575} decreased with increasing ALP concentration, and this decrease was found to be linear in the ALP concentration range of 0.8–16 U/L (Fig. 4A). The limit of detection (LOD = 3S/K, where S is the standard deviation of the blank signal and K is the slope of the standard curve) was calculated as 0.78 U/L. A relative standard deviation (RSD) of 1.19% was obtained from six replicated measurements of a 2 U/L ALP sample, which was indicative of good reproducibility. Table S1 summarized some fluorescent approaches for ALP determination. It can be seen that our method is more sensitive than most listed methods.

The presence of complex proteins in biological systems results in a high demand for selectivity improvement through the use of enzyme-triggered reactions in biological and clinical applications. To evaluate the specificity of the proposed fluorescent ALP biosensor, eight common enzymes (proteinase K, catalase, glucose oxidase, horseradish peroxidase, lysozyme, urease, acetylcholinesterase, and

superoxide dismutase) were investigated. As shown in Fig. 4B, these enzymes caused no obvious fluorescence change despite being present at levels exceeding that of ALP 10- to 100-fold, which was indicative of good selectivity for ALP.

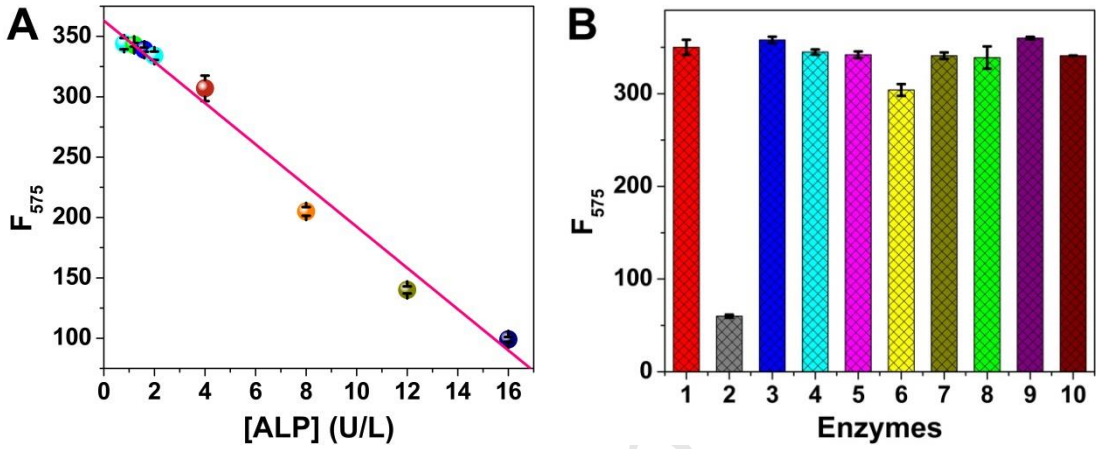

Fig. 4. (A) Linear relationship between F_{575} and ALP concentration. (B) Selectivity of the ALP sensing system. The order of 1–10 corresponds to blank, alkaline phosphatase (ALP), proteinase K, catalase, glucose oxidase, horseradish peroxidase, lysozyme, urease, acetylcholinesterase, and superoxide dismutase. The concentration of alkaline phosphatase equaled 20 U/L, that of acetylcholinesterase equaled 200 U/L, and those of other enzymes equaled 2000 U/L.

3.4. ALP assay in human osteosarcoma cells

As ALP is a ubiquitous intracellular enzyme, and its activity is an indicator of osteoblast differentiation, this enzyme is widely used in the clinical research of bone metabolism abnormalities and osteopathy. Therefore, the quantitative detection of intracellular ALP activity is of high clinical significance. However, because of the influence of cell culture medium, cell density, cell state, and cell lysate, the detection of intracellular ALP activity is more demanding than that of serum. To verify the applicability of the developed method to complex sample analysis, it was used to determine the level of ALP in Saos-2 human osteosarcoma cells, and the results were shown to be well linearly correlated (r=0.991) with those of the *p*-nitrophenyl phosphate (PNPP) method (Fig. 5). Notably, the difference of measured ALP

concentration between the two approaches is ascribed to the different kinetic parameters of ALP towards PPi and PNPP. In a further spike-in recovery experiment, quantitative detection of ALP was achieved with an acceptable recovery of 90.5−111.4% (Table 1) and an RSD of <5%, which showed that the developed method is suitable for the detection of ALP in complex biological samples and exhibits satisfactory accuracy and precision.

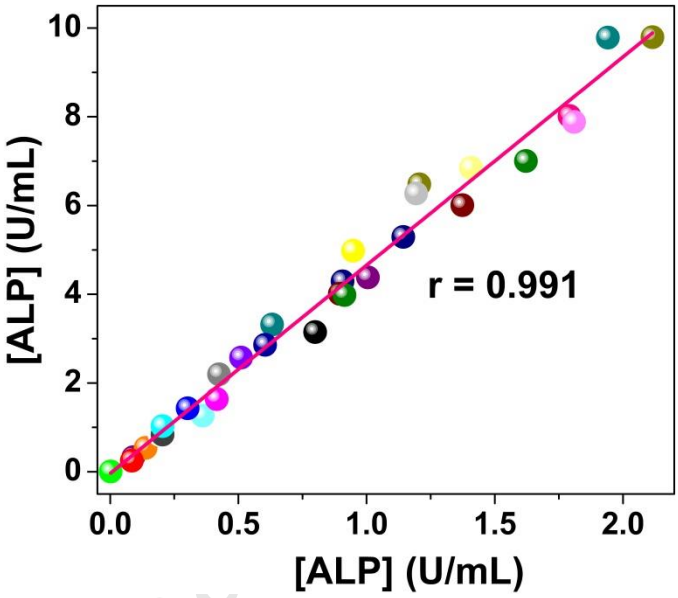

Fig. 5. Correlation between BSA/MPA-AuNCs (x-axis) and PNPP (y-axis) methods for the determination of ALP content in Saos-2 cells.

Table 1. Results of the spike-in recovery experiment for ALP quantitation in Saos-2 cells.

Spiked (U/L)	Found (U/L)	Recovery (%)	RSD (%, n=4)
0	2.5	–	–
2	4.7	111.4	1.95
4	6.1	90.5	2.94
5	7.1	91.3	3.37

3.5. Screening of ALP inhibitors

In view of the importance of enzyme inhibitor research for drug design, the

developed biosensor was employed to evaluate ALP inhibitor. As NaF is a common inhibitor of ALP [34], it was chosen as the target to verify the applicability of the enzyme inhibitor screening procedure. NaF was pretested for its effect on the fluorescent intensity of our assay system. It was found that NaF can not cause any significant change in the fluorescent intensity of BSA/MPA-AuNCs-Fe^{3+}-PPi mixture (Fig. S1). Fig. 6 shows that ALP activity progressively decreased with increasing NaF concentration, with the half-inhibitory concentration determined as 0.52 mM. These results indicate that the sensing system is suited for ALP inhibitor screening.

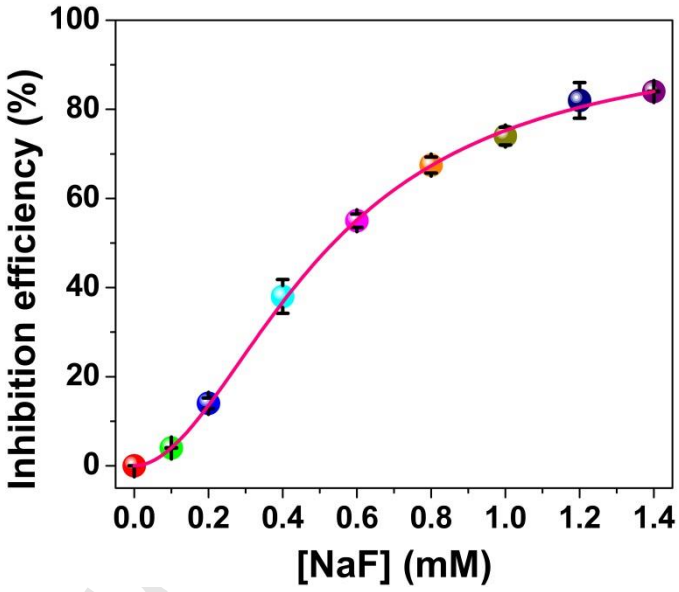

Fig. 6. Effect of NaF concentration on ALP inhibition efficiency.

4. Conclusion

Herein, we designed a fluorescence ALP sensor using PPi as a substrate, and Fe^{3+} as an effective quencher of BSA/MPA-AuNCs fluorescence. The Fe^{3+}-induced quenching of BSA/MPA-AuNCs fluorescence in combination with specific Fe^{3+}-PPi binding ability and the degradation of PPi by ALP allowed for ALP quantitation based on the turn-off-on-off signal as a readout. The developed method was successfully applied to the detection of ALP in human osteosarcoma cells and the study of the inhibitory effect of NaF on ALP activity. Therefore, the developed biosensor was concluded to have a broad range of potential applications in biological research, drug

discovery, and clinical medicine.

Acknowledgements

This work was supported by the National Natural Science Foundation of China (21675024, 21804021), the Program for Innovative Leading Talents in Fujian Province (2016B016), the Natural Science Foundation of Fujian Province (2019J01304), and the Science and Technology Project of Fujian Province (2018L3008).

References

[1] J.L. Ma, B.C. Yin, X. Wu, B.C. Ye, Copper-mediated DNA-scaffolded silver nanocluster on-off switch for detection of pyrophosphate and alkaline phosphatase, Anal. Chem. 88 (2016) 9219–9125.

[2] A.K. Sharma, S. Pandey, M.S. Khan, H.F. Wu, Protein stabilized fluorescent gold nanocubes as selective probe for alkaline phosphatase via inner filter effect, Sens. Actuators B 259 (2018) 83–89.

[3] K. Ooi, K. Shiraki, Y. Morishita, T. Nobori, High-molecular intestinal alkaline phosphatase in chronic liver diseases, J. Clin. Lab. Anal. 21 (2007) 133–139.

[4] P. Garnero, P.D. Delmas, Assessment of the serum levels of bone alkaline-phosphatase with a new immunoradiometric assay in patients with metabolic bone-disease, J. Clin. Endocr. Metab. 77 (1993) 1046–1053.

[5] S.R. Rao, A.E. Snaith, D. Marino, X. Cheng, S.T. Lwin, I.R. Orriss, et al., Tumour-derived alkaline phosphatase regulates tumour growth, epithelial plasticity and disease-free survival in metastatic prostate cancer, Br. J. Cancer 116 (2017) 227–236.

[6] C.M. Ruan, W. Wang, B.H. Gu, Detection of alkaline phosphatase using surface-enhanced Raman spectroscopy, Anal. Chem. 78 (2006) 3379–3384.

[7] D.E. Wang, X.H. Gao, G.B. Li, T. Xue, H. Yang, H.Y. Xu, Facile colorimetric assay of alkaline phosphatase activity using polydiacetylene liposomes with calcium ions and pyrophosphate, Sens. Actuators B 289 (2019) 85–92.

[8] Y.Q. Liu, E.H. Xiong, X.Y. Li, J.J. Li, X.H. Zhang, J.H. Chen, Sensitive electrochemical assay of alkaline phosphatase activity based on TdT-mediated hemin/G-quadruplex DNAzyme nanowires for signal amplification, Biosens. Bioelectron. 87 (2017) 970–975.

[9] L. Shang, S.J. Dong, G.U. Nienhaus, Ultra-small fluorescent metal nanoclusters: Synthesis and biological applications, Nano Today 6 (2011) 401–418.

[10] M. Zhu, C.M. Aikens, F.J. Hollander, G.C. Schatz, R. Jin, Correlating the crystal structure of A thiol-protected Au_{25} cluster and optical properties, J. Am. Chem. Soc. 130 (2008) 5883–5885.

[11] M.Z. Zhu, C.M. Aikens, M.P. Hendrich, R. Gupta, H.F. Qian, G.C. Schatz, et al., Reversible switching of magnetism in thiolate-protected Au-25 superatoms, J. Am. Chem. Soc. 131 (2009) 2490–2492.

[12] C.J. Zeng, T. Li, A. Das, N.L. Rosi, R.C. Jin, Chiral structure of thiolate-protected 28-gold-atom nanocluster determined by x-ray crystallography, J. Am. Chem. Soc. 135 (2013) 10011–10013.

[13] G.L. Wang, L.Y. Jin, Y.M. Dong, X.M. Wu, Z.J. Li, Intrinsic enzyme mimicking activity of gold nanoclusters upon visible light triggering and its application for colorimetric trypsin detection, Biosens. Bioelectron. 64 (2015) 523–529.

[14] J. Xie, Y. Zheng, J.Y. Ying, Protein-directed synthesis of highly fluorescent gold nanoclusters, J. Am. Chem. Soc. 131 (2009) 888–889.

[15] H.H. Deng, X.Q. Shi, F.F. Wang, H.P. Peng, A.L. Liu, X.H. Xia, et al., Fabrication of water-soluble, green-emitting gold nanoclusters with a 65% photoluminescence quantum yield via host-guest recognition, Chem. Mater. 29 (2017) 1362–1369.

[16] L.L. Li, H.Y. Liu, Y.Y. Shen, J.R. Zhang, J.J. Zhu, Electrogenerated chemiluminescence of Au nanoclusters for the detection of dopamine, Anal. Chem. 83 (2011) 661–665.

[17] H.P. Peng, Z.N. Huang, Y.L. Sheng, X.P. Zhang, H.H. Deng, W. Chen, et al., Pre-oxidation of gold nanoclusters results in a 66% anodic electrochemiluminescence yield and drives mechanistic insights, Angew. Chem. Int. Ed. 58 (2019) 11691–11694.

[18] X. Wu, X.X. He, K.M. Wang, C. Xie, B. Zhou, Z.H. Qing, Ultrasmall near-infrared gold nanoclusters for tumor fluorescence imaging in vivo, Nanoscale 2 (2010) 2244–2249.

[19] Y.L. Liu, K.L. Ai, X.L. Cheng, L.H. Huo, L.H. Lu, Gold-nanocluster-based fluorescent sensors for highly sensitive and selective detection of cyanide in water, Adv. Funct. Mater. 20 (2010) 951–956.

[20] H. Kawasaki, K. Hamaguchi, I. Osaka, R. Arakawa, pH-Dependent synthesis of pepsin-mediated gold nanoclusters with blue green and red fluorescent emission, Adv. Funct. Mater. 21 (2011) 3508–3515.

[21] J.A.A. Ho, H.C. Chang, W.T. Su, DOPA-mediated reduction allows the facile synthesis of fluorescent gold nanoclusters for use as sensing probes for ferric ions, Anal. Chem. 84 (2012) 3246–3253.

[22] L. Shang, S. Brandholt, F. Stockmar, V. Trouillet, M. Bruns, G.U. Nienhaus, Effect of protein adsorption on the fluorescence of ultrasmall gold nanoclusters, Small 8 (2012) 661–665.

[23] L. Shang, F. Stockmar, N. Azadfar, G.U. Nienhaus, Intracellular thermometry by using fluorescent gold nanoclusters, Angew. Chem. Int. Ed. 52 (2013) 11154–11157.

[24] M. Zhuang, C.Q. Ding, A.W. Zhu, Y. Tian, Ratiometric fluorescence probe for monitoring hydroxyl radical in live cells based on gold nanoclusters, Anal. Chem. 86 (2014) 1829–1836.

[25] V. Venkatesh, A. Shukla, S. Sivakumar, S. Verma, Purine-stabilized green fluorescent gold nanoclusters for cell nuclei imaging applications, ACS Appl. Mater. Interfaces 6 (2014) 2185–2191.

[26] H.H. Deng, G.W. Wu, Z.Q. Zou, H.P. Peng, A.L. Liu, X.H. Lin, et al., pH-Sensitive gold nanoclusters: preparation and analytical applications for urea, urease, and urease inhibitor detection, Chem. Commun. 51 (2015) 7847–7850.

[27] J.Y. Yang, T. Yang, X.Y. Wang, M.L. Chen, Y.L. Yu, J.H. Wang, Mercury speciation with fluorescent gold nanocluster as a probe, Anal. Chem. 90 (2018) 6945–6951.

[28] M. Jayasree, R.S. Aparna, R.R. Anjana, J.S.A. Devi, N. John, K. Abha, et al.,

Fluorescence turn on detection of bilirubin using Fe(III) modulated BSA stabilized copper nanocluster; A mechanistic perception, Anal. Chim. Acta 1031 (2018) 152–160.

[29] A. Martin-Barreiro, S. de Marcos, J.M. de la Fuente, V. Grazu, J. Galban, Gold nanocluster fluorescence as an indicator for optical enzymatic nanobiosensors: choline and acetylcholine determination, Sens. Actuators B 277 (2018) 261–270.

[30] K.Y. Huang, H.X. He, S.B. He, X.P. Zhang, H.P. Peng, Z. Lin, et al., Gold nanocluster-based fluorescence turn-off probe for sensing of doxorubicin by photoinduced electron transfer, Sens. Actuators B 296 (2019) 126656.

[31] H.H. Deng, F.F. Wang, X.Q. Shi, H.P. Peng, A.L. Liu, X.H. Xia, et al., Water-soluble gold nanoclusters prepared by protein-ligand interaction as fluorescent probe for real-time assay of pyrophosphatase activity, Biosens. Bioelectron. 83 (2016) 1–8.

[32] H.H. Deng, F.F. Wang, Y.H. Liu, H.P. Peng, K.L. Li, A.L. Liu, et al., Label-free, resettable, and multi-readout logic gates based on chemically induced fluorescence switching of gold nanoclusters, J. Mater. Chem. C 4 (2016) 7141–7147.

[33] T. Zhang, H.L. Fan, G.L. Liu, J. Jiang, J.G. Zhou, Q.H. Jin, Different effects of Fe^{2+} and Fe^{3+} on conjugated polymer $PPESO_3$: a novel platform for sensitive assays of hydrogen peroxide and glucose, Chem. Commun. (2008) 5414–5416.

[34] C. Shen, X. Li, A. Rasooly, L. Guo, K. Zhang, M. Yang, A single electrochemical biosensor for detecting the activity and inhibition of both protein kinase and alkaline phosphatase based on phosphate ions induced deposition of redox precipitates, Biosen. Bioelectron. 85 (2016) 220–225.

Author Contribution Statement

Hao-Hua Deng: Conceptualization, Methodology, Writing - Original Draft.

Qi Deng: Methodology, Investigation, Validation.

Ke-Lin Li: Investigation, Visualization.

Qiong-Qiong Zhuang: Investigation.

Yu-Bin Zhuang: Investigation.

Hua-Ping Peng: Supervision, Writing - Review & Editing.

Xing-Hua Xia: Supervision.

Wei Chen: Conceptualization, Supervision, Writing - Review & Editing.

Declaration of interests

☒ The authors declare that they have no known competing financial interests or personal relationships that could have appeared to influence the work reported in this paper.

☐The authors declare the following financial interests/personal relationships which may be considered as potential competing interests:

Graphical abstract

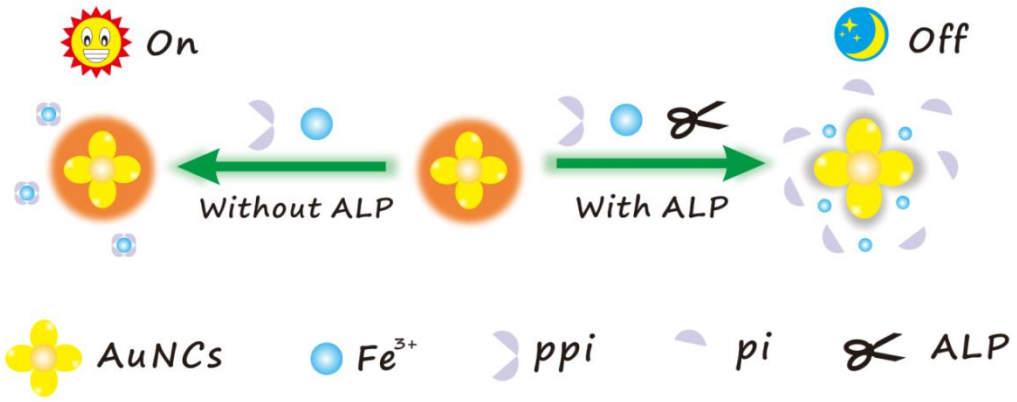

Highlights

- Alkaline phosphatase detection in human osteosarcoma cells.
- BSA/3-mercaptopropionic acid co-modified AuNC as a fluorescence probe.
- Fe^{3+}-induced quenching of BSA/MPA-AuNC fluorescence.
- Pyrophosphate as an alkaline phosphatase substrate and Fe^{3+} chelator.